

SPREADING CORTICAL DEPOLARIZATION



Spreading Diffusion-Restriction Events in the Gyrencephalic Brain After Subarachnoid Hemorrhage Revealed by Continuous Magnetic Resonance Imaging

Jed A. Hartings^{1*} , Christopher P. Carroll^{2,3} and Gregory Lee⁴

© 2021 Springer Science+Business Media, LLC, part of Springer Nature and Neurocritical Care Society

Abstract

Background: How widely spreading depolarizations (SDs) propagate through the gyrencephalic brain, including sulci and deeper cortical areas, remains an important clinical question. Here, we investigated SDs that occur spontaneously after subarachnoid placement of autologous blood clots in sulci of the juvenile swine brain.

Methods: To investigate the three-dimensional spread of waves, animals underwent continuous diffusion-weighted magnetic resonance imaging (DW-MRI) for up to 6 h following clot placement. SD is the mechanism of the cytotoxic edema of developing infarction that is diagnosed by DW-MRI, and DW-MRI also captures transient diffusion restriction caused by SD in less injured or healthy brains. Here, images ($b = 0, 375, \text{ and } 750$) were acquired across five coronal slices with 1.25×1.25 -mm in-plane resolution and 5-mm slice thickness, and the protocol was repeated every 6.83–9.15 s. Spatial drift correction, temporal smoothing, and signal intensity normalization were applied to generate videos of diffusion signal intensity changes for each coronal slice.

Results: Review of video data from five animals revealed ten discrete events consisting of focal diffusion restriction that propagated through cerebral cortex. All events originated in the cortex surrounding the sulcal clot, either in the gyrus ($n = 4$) or in the sulcal depth ($n = 6$). In six cases, two to three independent waves spread simultaneously in medial, lateral, and antero–posterior directions. Waves traveled within sulcal walls, traversed the depths of sulci to re-emerge on the adjacent gyrus, and, in three cases, spread fully around the dorsolateral convexity. One event spread deep to olfactory regions along midline cortex, and no events were observed contralateral to the subarachnoid clot.

Conclusions: Together, these results suggest that SDs in the injured gyrencephalic brain originate near the injury focus and can spread extensively through the cortex to wide and deep uninjured regions. These findings have implications for transient neurologic deficits in the neurocritically ill patient and relevance to patient monitoring and therapeutics.

Keywords: Spreading depolarization, Spreading depression, Subarachnoid hemorrhage, Brain injury, Magnetic resonance imaging, Diffusion restriction, Swine, Gyrencephalic

Introduction

Spreading depolarizations (SDs) propagate through cerebral gray matter unlike any other physiologic or pathologic activity. Conveyed through bulk diffusion in the extracellular space, they follow the nonlinear dynamic behavior of a reaction–diffusion process in an excitable medium. Thus, they can propagate through cerebral cortex as radial, semiplanar, and spiral waves, cycle in reentrant loops, break up into child waves, or collide and

*Correspondence: jed.hartings@uc.edu

¹ Department of Neurosurgery, University of Cincinnati College of Medicine, Cincinnati, OH, USA

Full list of author information is available at the end of the article

This article is part of the collection “Spreading Cortical Depolarization.”

annihilate each other. The patterns are dependent on anatomic features (veins, sulci, and boundaries), functional blocks (lesions or refractory periods), and tissue cytoarchitecture. These patterns and factors have been well documented in recent imaging studies of lissencephalic rodent and gyrencephalic swine brains [1–3], demonstrating that prior notions of SD propagation in homogenous radial patterns are more the exception than the rule. These imaging studies provide insight into SD mechanisms and help explain the complex patterns of SDs observed in patients with acute brain injury. When recording from linear electrode arrays placed along the surface of the gyrencephalic brain, SDs usually have complex patterns characterized by repetitive occurrence, direction reversals, branching, and variable time delays between electrodes.

Despite these advances, several important questions about SD propagation require further investigation. For instance, it is unknown how far SDs may propagate, as electrode strips in patients only cover 5 linear centimeters of the brain surface. A related question is the extent to which SDs can propagate through the depths of a sulcus to reemerge on the adjacent gyrus. A potential method to address these questions is diffusion-weighted magnetic resonance imaging (DW-MRI), which can be applied in different imaging planes throughout the brain. The basis for DW-MRI of SDs is that the breakdown of physiological ion gradients during SD drives a massive water influx into cells, causing neuronal swelling, dendritic beading, and 50% shrinkage of the extracellular space [4, 5]. These changes are known as cytotoxic edema, which is observed during SD by electron microscopy [6, 7] and in vivo two-photon imaging [8, 9]. They can also be observed by using magnetic resonance imaging (MRI) as restricted water diffusion because the edema restricts intracellular and extracellular water movement. DW-MRI has been used to image the propagation of SD in lissencephalic [10–12] and gyrencephalic [13] brains and to study the role of SD in ischemic stroke and subarachnoid hemorrhage [14–17]. In the core of a focal ischemic lesion, depolarization and diffusion restriction are persistent unless blood flow is restored. In the periphery of a normally perfused brain, diffusion changes are transient because SD recovers spontaneously after 1–2 min.

Here we used a previously developed swine model of subarachnoid hemorrhage to investigate SD propagation throughout the three-dimensional structure of the gyrencephalic brain [18]. In our prior study, clotted or fresh autologous blood was injected in a frontal sulcus, and spontaneous repetitive SDs were observed in many animals by using electrocorticography in association with developing cortical infarcts. Here, DW-MRI was used to

identify and track spreading diffusion changes associated with SDs.

Methods

We used the same protocol previously reported with slight variations, as approved by the Institutional Animal Care and Use Committee at Cincinnati Children's Hospital Medical Center (CCHMC) [18]. In brief, anesthesia was induced with intramuscular Telazol (5 mg/kg) and xylazine (1 mg/kg), animals were intubated and mechanically ventilated with 30% O₂, and anesthesia was maintained with ~2% isoflurane during initial procedures of catheter placement and physiologic monitoring preparation. Anesthesia was then switched to intravenous propofol with a 3 ml/kg bolus followed by continuous infusion at 15–25 mg/kg/hr, and a craniotomy was performed over the superior frontal and motor gyri, with durotomy and arachnoid dissection as described previously. Animals were then transferred to the MRI suite and subarachnoid hemorrhage was modeled by placing 1.5 ml of clotted and 1.0 ml of fresh blood into the cruciate sulcus between superior frontal and motor gyri. After closure, monitoring of temperature (38.4 ± 0.7 °C), mean arterial pressure (92 ± 17 mm Hg), and E_TCO₂ (40 ± 9 mm Hg) was discontinued and animals were rapidly transferred into the MRI coil to begin imaging 14 (± 8) minutes after clot placement. Throughout imaging, animals were cooled with a fan and maintained with lactated ringers (50 ml/hr) and propofol anesthesia.

Imaging was conducted on a 1.5-T scanner equipped with a surface receiver coil placed just above the cranial window. Structural sequences were acquired every 2 h from the start until animal was killed at 6 h. Between structural scans, a DW-MRI protocol was repeated continuously in three blocks lasting ~100 min each. The spatial field of view of the DW-MRI acquisitions was $100 \times 100 \times 25$ mm and was collected with 1.25×1.25 mm resolution in-plane across five adjacent slices (5 mm thick). The protocol used diffusion weightings of $b=0$, $b=375$, and $b=750$ s/mm², in which the $b=375$ and $b=750$ images were averages of the diffusion weighting across three orthogonal directions. Images were read out using a standard spin-echo echo-planar-imaging protocol with TE=80 ms. This protocol produced a set of multislice images obtained at DW-MRI ($b=0$, $b=375$, $b=750$) every 6.83 to 9.15 s, depending on minor protocol variations. Thus, we were able to observe contrast changes at a temporal resolution of <10 s over a period of hours.

In processing images, no spatial smoothing was applied. However, a slow drift in the spatial position of the brain was apparent over the course of an experiment, likely due to a small temporal drift in the main magnetic

field that accompanies gradient heating over the course of several hours. To correct for this, DW-MRI time series were coregistered to T2-weighted structural images by using Motion Correction using FMRIB's Linear Image Registration Tool (MC-FLIRT) as implemented in the Oxford Centre for Functional Magnetic Resonance Imaging of the Brain (FMRIB) Software Library [19, 20]. Reference DW-MRI time points at $b=0$ were coregistered by using FMRIB Software Library's FLIRT (FMRIB's Linear Image Registration Tool). Additionally, to improve the signal-to-noise ratio, images at diffusion weightings of $b=0$, $b=375$, and $b=750$ were averaged and then temporally smoothed with a Gaussian function having a full-width-at-half-max of eight temporal frames. This level of temporal smoothing was chosen to reduce noise while not exceeding the expected duration of a depolarization wave at a given point in the brain. To remove the effects of very slow long-term temporal drift in signal intensity, the time series was normalized by division by a baseline intensity at each time point. This baseline intensity was obtained by creating a version of the time series with a much broader temporal smoothing (full-width-at-half-max of 128 time points). This broad temporal smoothing was chosen to be substantially longer than a depolarization's duration. The final intensities are thus a ratio of the (b -value averaged) diffusion signal to the baseline, and images represent qualitative mean intensity changes shown on the viridis color scale, in which an increase in DW-MRI intensity reflects an underlying reduction in diffusion. For visual inspection, images were coded on a viridis color scale and stitched together serially in a video sequence. In general, the data were too noisy to reliably fit time-resolved quantitative values for the apparent diffusion coefficient at the spatial resolution used.

Results

Five female juvenile swine (48 ± 3 kg) were studied. The review of continuous imaging data revealed ten discrete events consisting of focal diffusion restriction that propagated through the cerebral cortex. There were two, four, and four events in three animals, respectively, and none in the other two. All ten events originated in the cortex surrounding the sulcal clot. Six originated in the wall or depth of the sulcus (Fig. 1) and three originated at the adjacent gyrus. In some cases, there appeared to be multiple sites of origin within the sulcus. After initiation, events generally showed spread through the cortex surrounding the clot, encompassing medial and lateral walls of the sulcus (Fig. 1). In six cases, 2–3 independent waves were observed traveling in different directions, typically medially and laterally through the parietal lobe, but also in anterior–posterior directions. The pattern of spread was circuitous, obeyed anatomic boundaries, and

appeared mainly to follow the cerebral cortex. Specifically, there was evidence of spread within a sulcus along both anterior–posterior and ventral–dorsal axes. In some cases, the waves clearly traveled into a sulcus and emerged at the opposite gyrus to continue further spread across substantial cortical regions. Lateral and then ventral spread around the convexity reached the Rhinal fissure in three cases but did not continue beyond this structure (Fig. 2). One event was remarkable in its ventral propagation along two separate paths, including cortex adjacent to midline, down to the olfactory region (Supplemental Video 1). For two animals, we calculated the propagation velocities for diffusion restriction changes at various points along the cortical mantle where they could be reliably measured and tracked. Velocities were 2.90 ± 1.23 mm/min (mean \pm standard deviation; $n=8$ segments) and 1.91 ± 0.48 mm/min ($n=6$ segments) and were based on the measurement of 7.6 ± 3.0 mm and 5.7 ± 1.7 mm of spread, respectively. No events were observed to originate in, or spread to, the hemisphere contralateral to the subarachnoid clot.

Animals were killed after imaging and brains were harvested for 2,3,5-triphenyltetrazolium chloride (TTC) assessment of infarction. Lesions consisted of full or patchy infarction through the cortex adjacent to the subarachnoid clot, with some cases of petechial hemorrhage, as reported previously [18]. Maximal sulcal clot thickness ranged from 2.7 to 6.8 mm. Cortical infarct volumes assessed through serial sections ranged 54–615 mm³.

Discussion

The earliest studies in the gyrencephalic brain suggested that SDs are capable of propagating through a sulcus to emerge at the adjacent gyrus, but also that they often terminated within the sulcus [21, 22]. The most striking evidence is derived from the brain surface imaging study of Santos et al. [2], in which SDs are shown to emerge from a sulcus and then engulf the gyral crest (e.g., their Supplemental Video 6). Similarly, with laser speckle imaging of the human brain after decompressive hemicraniectomy for stroke, Woitzik et al. [23] observed two SDs passed from one gyrus to another through the sulci. Nonetheless, the predominant finding from both studies was that most SDs preferentially spread along the gyri, avoiding sulci as anatomic barriers that appear less conducive to propagation. An extreme example of this behavior is the repetitive cycling of SD through the gyri surrounding an isolated sulcus. Moreover, the clinical study found that SDs were often terminated when they reached a sulcus.

Except for one study using magnetoencephalography [21], these prior studies have all used surface imaging of the brain to study SD propagation. Here, we used a different approach of DW-MRI that allowed for

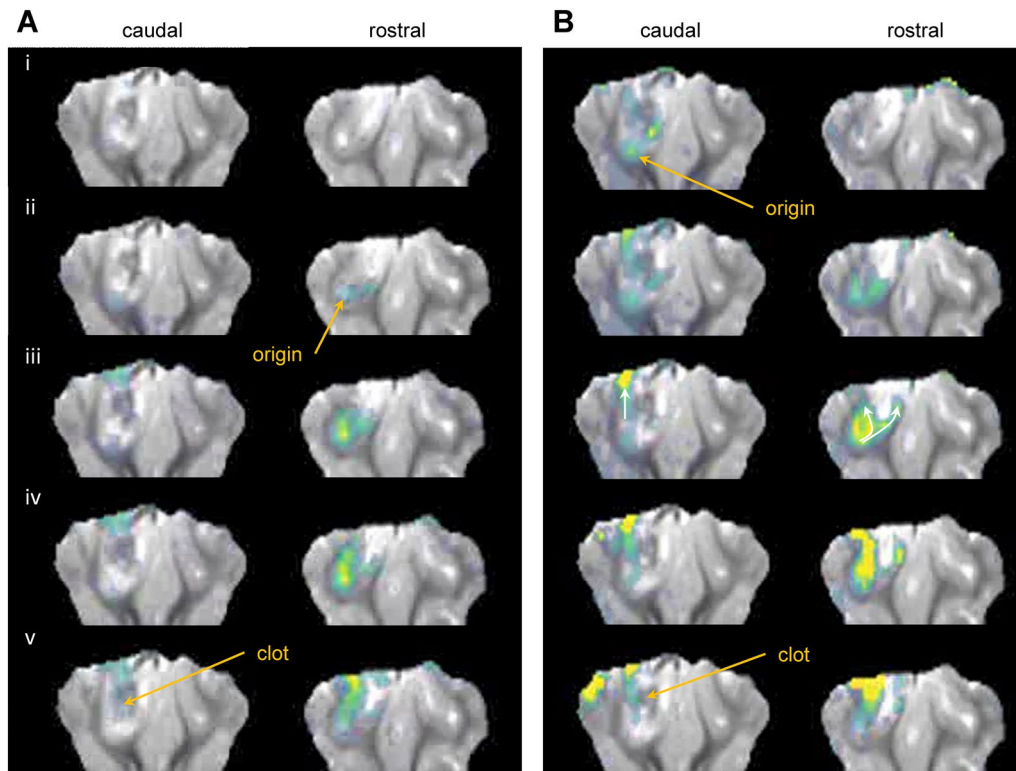


Fig. 1 Origin and spread of diffusion restriction events within sulcus. Each panel shows a time series through two coronal slices, rostral and caudal, separated by 5 mm. ADC maps were color coded using the viridis scale and were overlaid on the corresponding high-resolution (0.28×0.28 mm) T2-weighted anatomic scans after coregistration according to anatomic landmarks. **A**, This event begins 4 h after clot placement, originating at the bottom of the coronal sulcus in which the clot is placed, appearing in the most rostral slice (right). From initiation (ii), it spreads dorsally (iii–iv) and then laterally (v) as it crests the gyrus. Little or no spread is seen through the medial wall or in the more caudal slice, which shows hyperintensity throughout the sulcal cortex surrounding the clot. **B**, This episode in the same animal begins 2 h after clot placement with several hotspots. Those along the lateral wall coalesce and spread from the bottom of the sulcus to the gyrus, then traverse the adjacent sulcus to reach the dorsolateral convexity, as seen in the caudal slice sequence (left). The same wave simultaneously spreads to the more rostral slice (right) in the depth of the sulcus before splitting to propagate up along medial and lateral sulcal walls to the gyral crests. ADC, apparent diffusion coefficient

monitoring throughout the coronal plane, into sulcal depths, and across multiple planes on the anterior–posterior axis. Our results confirm that SDs can propagate through sulci and, further, they provide compelling evidence that SDs are capable of widespread propagation throughout the gyrencephalic brain. Individual events were observed to spread through sulci both from the surface to the depths, and reverse, as well as on the anterior–posterior axis within a sulcus. Further, they were observed to propagate medially and laterally along the dorsolateral surface of the brain and into the deep cortex. In some cases, this was accomplished through the split of one SD into multiple waves that spread simultaneously in different directions. On the other hand, SDs did not spread beyond the Rhinal fissure, which appears to be a hard boundary analogous to the parieto-occipital sulcus in human migraineurs [24].

Whether widespread propagation is the rule or the exception is unknown, as the sample size of our study was small and the detection methods used may have been biased toward more conspicuous, widely spreading events. Thus, it is possible that some SDs in these experiments escaped detection. Indeed, the number of SDs observed was rather limited compared with those observed in the same swine model using electrocorticographic monitoring [18]. Another factor that may have limited detection was the use of coronal imaging for acquisition and data visualization. Other planes more focused on surface gyri may have revealed additional events spreading preferentially in the anterior–posterior axis. Thus, a general shortcoming of this study was the lack of a gold standard technique for comparison. Nonetheless, the events identified exhibited the hallmark propagation velocity of SD and could not be reasonably attributed to other known phenomena.

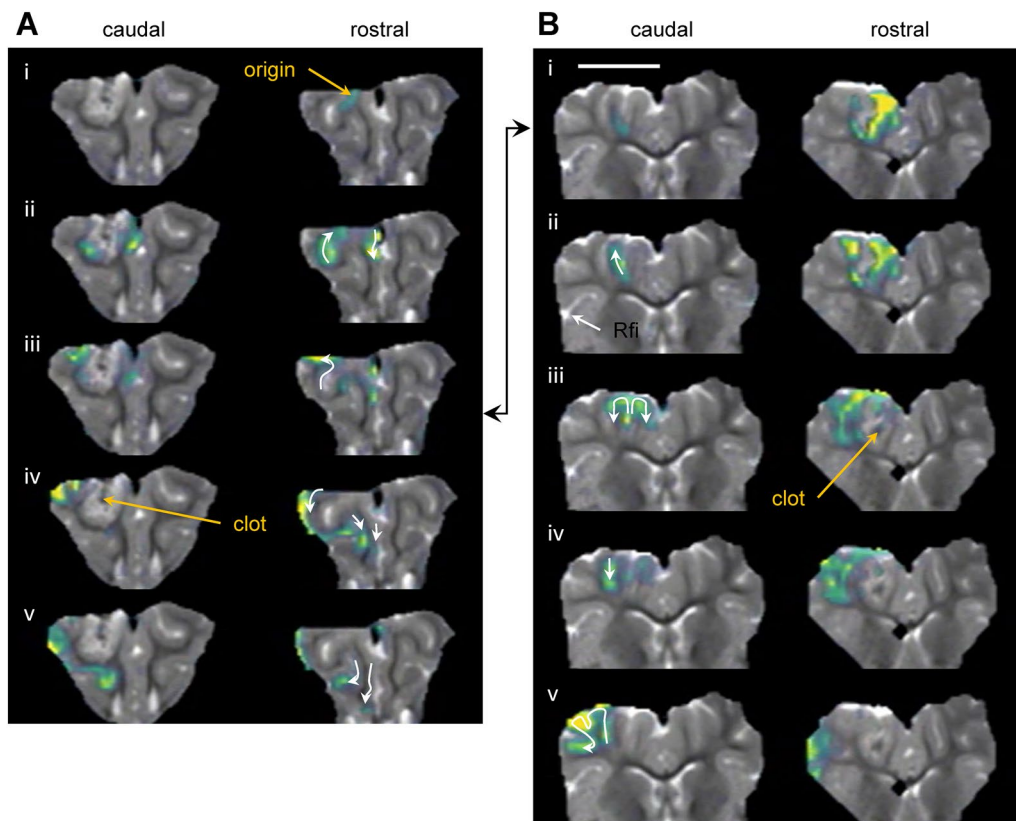


Fig. 2 Widespread propagation of spreading diffusion restriction. Conventions are the same as in Fig. 1, showing a sequence beginning 2 h after clot placement in a different animal. **A**, The sequence originates at the medial gyral crest adjacent to the clot sulcus (i, rostral) and then spreads as two separate waves along medial and lateral paths. On the lateral path, the wave spreads down into the clot sulcus, continuing to posterior slices within the sulcus, and further laterally around the convexity to terminate at the Rhinal fissure. On the medial path, the wave follows the cortex inferiorly along the midline, ending in the olfactory region (ii–v). A third event of an unknown source also arises in the insular cortex deep in the brain, moving inferiorly and then laterally along the cortical fold. **B**, This sequence depicts more posterior slices for the same events that are shown in **A**. Images in **B-i** are from the same time as those in **A-iii** and show the posterior spread of the original event to envelop the entire sulcal cortex medial to the clot (**B-i**, rostral). It then spreads within the sulcus to the more caudal slice and spreads up both sulcal walls within this slice (i–ii). The wave continues through gyri medially and laterally to spread into adjacent sulci (iii–iv), forming an “M” shape. It invades and traverses the several subsequent sulci (v) before eventually reaching the Rhinal fissure (Rfi) (not shown). See Supplemental Video 1 for the full event. Scale bar is 2 cm

Another important finding was that all SDs originated in the sulcal cortex adjacent to the subarachnoid clot. This was not surprising, as prior work in ischemic stroke has shown that SDs originate near the lesion focus on the penumbra [25, 26]. Nonetheless, this confirms the important clinical interpretation that SDs indicate a newly developing cortical lesion [27, 28], and the direction of spread could inform the location of the lesion (see Robinson et al., [29]). Indeed, postmortem staining confirmed cortical infarction in all animals of the present study. In future work, DW-MRI could be used similarly in this subarachnoid hemorrhage model to determine the time course of lesion development in relation to the occurrence of SDs. In the present study,

no attempts were made to do so. Finally, it is likely that the presence of blood throughout the sulcus was a facilitatory factor that promoted more widespread propagation within sulcal depths than what would otherwise be observed, for instance, in an uninjured brain. This consideration cautions against generalization of the present results to conditions such as migraine with aura.

Conclusions

In conclusion, our study demonstrates that SDs can propagate within and along sulci, widely throughout cortical areas, and deep in the brain, and that the occurrence of SDs is not restricted to the cortical surface where they are observed by electrocorticography in patients who are

neurocritically ill. These observations suggest the requisite conditions for the possible involvement of SDs in lesion development and transient neurologic deficits in tissue remote from the surface region of SD monitoring.

Supplementary Information

The online version contains supplementary material available at <https://doi.org/10.1007/s12028-021-01376-0>.

Author details

¹ Department of Neurosurgery, University of Cincinnati College of Medicine, Cincinnati, OH, USA. ² Department of Brain and Spinal Surgery, Naval Medical Center Portsmouth, Portsmouth, VA, USA. ³ Department of Surgery, Uniformed Services University, Bethesda, MD, USA. ⁴ Department of Radiology, Cincinnati Children's Hospital Medical Center, Cincinnati, OH, USA.

Author Contributions

JAH conceived the study, contributed to experimental design and execution, drafted the manuscript, and approval the final manuscript version. CPC contributed to experimental design, performed surgeries, collected data, edited the manuscript, and approved the final manuscript version. GL designed and executed the magnetic resonance imaging protocols, processed the data, analyzed results, contributed to manuscript preparation, and approved the final manuscript version.

Source of Support

This work was supported by the American Association of Neurological Surgeons/Congress of Neurological Surgeons (AANS/CNS) Joint Section on Cerebrovascular Surgery Robert J. Dempsey, MD, Cerebrovascular Research Award (to CPC) and the Mayfield Education and Research Foundation (to JAH, CPC).

Copyright Statement

Christopher P. Carroll, LCDR, MC, USN, is a military service member. This work was prepared as part of their official duties. Title 17 U.S.C. 105 provides that "Copyright protection under this title is not available for any work of the United States Government." Title 17 U.S.C. 101 defines a United States Government work as a work prepared by a military service member or employee of the United States Government as part of that person's official duties.

Disclaimer

The views expressed in this article reflect the results of research conducted by the authors and do not necessarily reflect the official policy or position of the Department of the Navy, Department of Defense, or United States Government.

Conflicts of Interest

The authors have no other conflicts to disclose.

Ethical Approval/Animal Rights

This study complies with all ethical guidelines and was conducted with approval and supervision of the institutional animal care and use committee.

Publisher's Note

Springer Nature remains neutral with regard to jurisdictional claims in published maps and institutional affiliations.

Received: 5 May 2021 Accepted: 8 October 2021

References

- Kaufmann D, Theriot JJ, Zyuzin J, et al. Heterogeneous incidence and propagation of spreading depolarizations. *J Cereb Blood Flow Metab.* 2016. <https://doi.org/10.1177/0271678X16659496>.
- Santos E, Scholl M, Sanchez-Porras R, et al. Radial, spiral and reverberating waves of spreading depolarization occur in the gyrencephalic brain. *Neuroimage.* 2014;99C:244–55.
- Santos E, Sanchez-Porras R, Sakowitz OW, et al. Heterogeneous propagation of spreading depolarizations in the lissencephalic and gyrencephalic brain. *J Cereb Blood Flow Metab.* 2017;37:2639–43.
- Dreier JP, Lemale CL, Kola V, et al. Spreading depolarization is not an epiphenomenon but the principal mechanism of the cytotoxic edema in various gray matter structures of the brain during stroke. *Neuropharmacology.* 2018;134:189–207.
- Hartings JA, Shuttleworth CW, Kirov SA, et al. The continuum of spreading depolarizations in acute cortical lesion development: examining Leao's legacy. *J Cereb Blood Flow Metab.* 2017;37:1571–94.
- Van Harrevelde A, Khattab FI. Changes in cortical extracellular space during spreading depression investigated with the electron microscope. *J Neurophysiol.* 1967;30:911–29.
- Kirov SA, Fomitcheva IV, Sword J. Rapid neuronal ultrastructure disruption and recovery during spreading depolarization-induced cytotoxic edema. *Cereb Cortex.* 2020;30:5517–31.
- Murphy TH, Li P, Betts K, et al. Two-photon imaging of stroke onset in vivo reveals that NMDA-receptor independent ischemic depolarization is the major cause of rapid reversible damage to dendrites and spines. *J Neurosci.* 2008;28:1756–72.
- Risher WC, Ard D, Yuan J, et al. Recurrent spontaneous spreading depolarizations facilitate acute dendritic injury in the ischemic penumbra. *J Neurosci.* 2010;30:9859–68.
- Latour LL, Hasegawa Y, Formato JE, et al. Spreading waves of decreased diffusion coefficient after cortical stimulation in the rat brain. *Magn Reson Med.* 1994;32:189–98.
- de Crespigny A, Rother J, van Bruggen N, et al. Magnetic resonance imaging assessment of cerebral hemodynamics during spreading depression in rats. *J Cereb Blood Flow Metab.* 1998;18:1008–17.
- Umesh Rudrapatna S, Hamming AM, Wermer MJ, et al. Measurement of distinctive features of cortical spreading depolarizations with different MRI contrasts. *NMR Biomed.* 2015;28:591–600.
- James MF, Smith MI, Bockhorst KH, et al. Cortical spreading depression in the gyrencephalic feline brain studied by magnetic resonance imaging. *J Physiol.* 1999;519(Pt 2):415–25.
- Busch E, Gyngell ML, Eis M, et al. Potassium-induced cortical spreading depressions during focal cerebral ischemia in rats: contribution to lesion growth assessed by diffusion-weighted NMR and biochemical imaging. *J Cereb Blood Flow Metab.* 1996;16:1090–9.
- Kastrup A, Neumann-Haefelin T, Moseley ME, et al. High speed diffusion magnetic resonance imaging of ischemia and spontaneous periinfarct spreading depression after thromboembolic stroke in the rat. *J Cereb Blood Flow Metab.* 2000;20:1636–47.
- Busch E, Beaulieu C, de Crespigny A, et al. Diffusion MR imaging during acute subarachnoid hemorrhage in rats. *Stroke.* 1998;29:2155–61.
- Yenari MA, Onley D, Hedehus M, et al. Diffusion- and perfusion-weighted magnetic resonance imaging of focal cerebral ischemia and cortical spreading depression under conditions of mild hypothermia. *Brain Res.* 2000;885:208–19.
- Hartings JA, York J, Carroll CP, et al. Subarachnoid blood acutely induces spreading depolarizations and early cortical infarction. *Brain.* 2017;140:2673–90.
- Jenkinson M, Smith S. A global optimisation method for robust affine registration of brain images. *Med Image Anal.* 2001;5:143–56.
- Jenkinson M, Bannister P, Brady M, et al. Improved optimization for the robust and accurate linear registration and motion correction of brain images. *Neuroimage.* 2002;17:825–41.
- Bowyer SM, Tepley N, Papuashvili N, et al. Analysis of MEG signals of spreading cortical depression with propagation constrained to a rectangular cortical strip. II. Gyrencephalic swine model. *Brain Res.* 1999;843:79–86.
- Sloan N, Jasper H. The identity of spreading depression and "suppression." *EEG Clin Neurophysiol.* 1950;2:59–78.
- Woitzik J, Hecht N, Pinczolits A, et al. Propagation of cortical spreading depolarization in the human cortex after malignant stroke. *Neurology.* 2013;80:1095–102.
- Hadjikhani N, Sanchez Del Rio M, Wu O, et al. Mechanisms of migraine aura revealed by functional MRI in human visual cortex. *Proc Natl Acad Sci U S A.* 2001;98:4687–92.

25. von Bornstadt D, Houben T, Seidel JL, et al. Supply-demand mismatch transients in susceptible peri-infarct hot zones explain the origins of spreading injury depolarizations. *Neuron*. 2015;85:1117–31.
26. Kumagai T, Walberer M, Nakamura H, et al. Distinct spatiotemporal patterns of spreading depolarizations during early infarct evolution: evidence from real-time imaging. *J Cereb Blood Flow Metab*. 2011;31:580–92.
27. Hartings JA. Spreading depolarization monitoring in neurocritical care of acute brain injury. *Curr Opin Crit Care*. 2017;23:94–102.
28. Dreier JP, Fabricius M, Ayata C, et al. Recording, analysis, and interpretation of spreading depolarizations in neurointensive care: review and recommendations of the COSBID research group. *J Cereb Blood Flow Metab*. 2017;37:1595–625.
29. Robinson D, Hartings J, Foreman B. First report of spreading depolarization correlates on scalp EEG confirmed with a depth electrode. *Neurocrit Care*. 2021;35(Suppl 2):100–4.